

Performance of Rotary Flow Cyclones

DAVID F. CILIBERTI

and

BRIAN W. LANCASTER

Chemical Engineering Department
Westinghouse Research Laboratories
Pittsburgh, Pennsylvania 15235

An analysis of the operation of the rotary flow cyclone suggests that no dust below 1μ will be captured in this equipment under normal operating conditions, and that performance will not deteriorate with the use of a dirty secondary flow. Experimental data support these conclusions.

SCOPE

Advanced power plants which utilize pressurized gases from coal gasification or fluidized bed combustion will require high efficiency dust collectors to protect gas turbine components from erosion. These collectors must be mechanically simple and capable of routine operation at high temperature and pressure.

A rotary flow cyclone collector has been developed, which, based on vendors data, shows the potential for

meeting these requirements. However, independent experimental data suggest that the unit performance may not always correspond to the vendors claims.

The work described in this paper was carried out to establish the operating characteristics of rotary flow cyclones and to determine if they may be useful in gas turbine, power plant applications.

CONCLUSIONS AND SIGNIFICANCE

A simple theoretical analysis of rotary flow cyclone operation implies that performance will be poorer than that reported by the manufacturers. Subsequent experimental work has failed to reproduce the high collection efficiencies which have been claimed for this equipment, and under our test conditions, performance has been no better than that of a similar sized unit of conventional design.

This leads us to the general conclusion that grade efficiency data for rotary flow cyclones are unreliable, and pilot scale testing is warranted before such equipment is installed.

More specifically, we conclude (with some regret) that rotary flow cyclones cannot be relied upon for the protection of gas turbines in advanced power plants.

THE ROTARY FLOW CYCLONE

A rotary flow cyclone consists of a cylindrical body into which two separate gas streams are introduced. The pri-

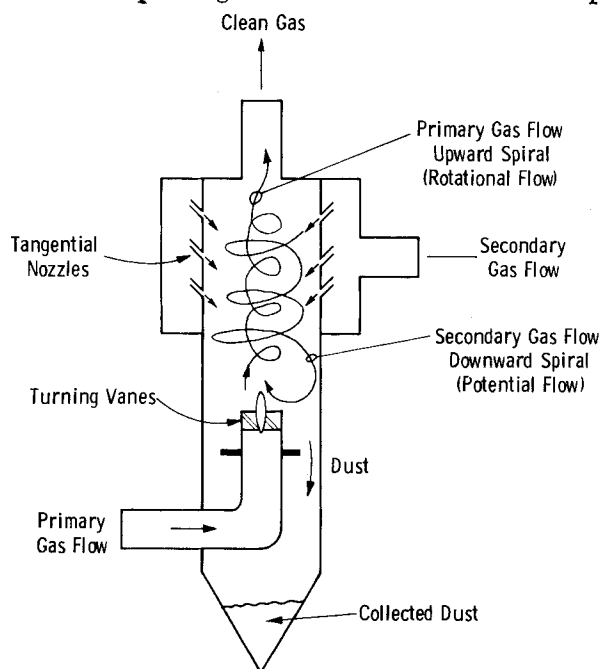


Fig. 1. Operation of a rotary flow cyclone.

mary flow, which is to be cleaned, enters through a central set of turning vanes located in the base of the unit. A secondary flow is introduced around the circumference of the unit at the top, either through tangential inlet nozzles (Figure 1) or through an annular set of turning vanes.

As particulates in the primary flow are thrown outwards toward the wall they are swept downward to the collection hopper by the secondary flow.

The physical principles of the cyclone are discussed in detail by Schmidt (1963). The unit is analyzed on the basis of an inner zone of rotational flow and an outer zone of potential flow. In comparing the rotary flow cyclone with a conventional reverse flow cyclone, Schmidt observes that short-circuiting of dirty gas from inlet to outlet is possible in the conventional unit but not in the rotary flow unit. This appears to be its major potential advantage.

In the experimental development of rotary flow cyclones, Klein (1963) relied heavily on a trial-and-error approach and made little use of any analytical results. The grade efficiency curve for a 200 mm diameter unit developed by Klein (1963) shows essentially complete collection at 5μ , with a cut point (50% collection) of 0.4μ .

Dunson (1970) determined the efficiency of rotary flow cyclones when operating on fly ash and on talc. The results with talc indicate a cut point of around 3μ , with little collection for particles below 2μ . Fly ash was col-

lected more efficiently than talc; however, the results do not allow a cut point to be established. Dunson suggests that agglomeration may be responsible for the difference in results obtained with different dusts. Lucas (1973) observes that Dunson's results are consistent with the performance of a conventional cyclone of comparable capacity and pressure drop.

Ogawa et al. (1972) made a detailed study of a rotary flow cyclone of their own design. An incorrect assumption in the relationship between radius and radial velocity invalidates their theoretical analysis; however, their experimental results are of particular interest. Under the most favorable operating conditions, a cut point of 3 μ was achieved, with essentially zero collection below 2 μ .

A SIMPLIFIED ANALYSIS

A simplified analysis of the rotary flow cyclone may be made based on two assumptions. First, rotational flow is assumed at any axial position in the core of the unit. Second, the secondary flow is assumed to enter the core uniformly, over the cylindrical bounding surface.

Consequently

$$v_t = \omega r \quad r \leq R_o \quad (1)$$

and

$$v_r = Q_s/2\pi R_o h, \quad r = R_o \quad (2)$$

To be captured, a particle must move from the central flow into the outer secondary flow. To achieve this, the centrifugal force on the particle at the boundary separating these two zones must overcome the drag force due to the inwardly directed radial gas velocity. Thus, by assuming Stokes law, the minimum particle size captured is given by

$$d = \sqrt{9\mu Q_s/\pi V_t^2 h\rho} \quad (3)$$

To obtain an estimate of V_t , the following angular momentum balance can be made on a section (length L) of the cylindrical core:

$$\frac{d}{dt}(I\omega) = \frac{dZ}{dt} \left(\frac{d}{dZ} \right) (I\omega) = \left(\frac{Q_s \rho L}{h} \right) (R_o \omega) (R_o) \quad (4)$$

since

$$I = (1/2)(\pi R_o^2 L \rho) (R_o^2) \quad (5)$$

and

$$\frac{dZ}{dt} = V_z = \left(1 + \frac{Q_s}{Q_p} \frac{Z}{h} \right) (Q_p)/R_o^2 \pi \quad (6)$$

Equation (4) can be integrated to yield

$$\omega(Z) = \omega_o \left\{ 1 + \frac{Z}{h} \frac{Q_s}{Q_p} \right\}^2 \quad (7)$$

To determine the initial value of ω , some assumptions must be made about the design of the cyclone. It would be possible, for example, to evaluate ω if the value of S for the cyclone were known. Various values of S have been

reported for high efficiency cyclones. Dalla Valla (1952) suggests a value of 3, while Friedlander et al. (1952) suggest 5. A value of 4 has been assumed here for rotary flow units. To use this information, consider the motion of the core section over the time increment dt :

$$dt = \frac{dZ}{V_z} = \frac{d\theta}{\omega} \quad (8)$$

If the values of $V_z(Z)$ from Equation (6) and $\omega(Z)$ from Equation (7) are substituted into Equation (8) and the resultant equation is integrated over the length of the cyclone, and through the angle of $2\pi S$, the following value for ω_o is obtained:

$$\omega_o = \left(\frac{2Q_p S}{h R_o^2} \right) \frac{1}{1 + \frac{Q_s}{Q_p} \cdot 1/2} \quad (9)$$

Consequently, the maximum value of V_T can be determined as

$$V_T(h) = R_o \omega(h) = \left(\frac{2S}{R_o h} \right) \frac{Q_p}{1 + \frac{Q_s}{Q_p} \frac{1}{2}} \left(1 + \frac{Q_s}{Q_p} \right)^2 \quad (10)$$

and substitutions of this value into (3) yield the minimum particle size capable of being captured:

$$d_o = \left(\frac{Q}{Q_T^2} \right) \left(\frac{3 R_o}{2S} \right) \sqrt{\frac{\mu Q_s h}{\pi \rho}} \quad (11)$$

Particles entering the cyclones in the primary flow will be subjected to centrifugal and drag forces. Making the usual assumptions, and equating the drag force to the centrifugal force, we can determine the radial velocity of the particle:

$$\frac{dr}{dt} = \left(\frac{dZ}{dt} \right) \left(\frac{dr}{dZ} \right) = \left(\frac{\rho d^2}{18\mu} \right) r \omega^2 \quad (12)$$

or

$$\frac{dr}{r} = \left(\frac{\rho d^2}{18\mu} \right) \left(\frac{\omega^2}{V_z} \right) dZ \quad (13)$$

By integration of the left term from an initial inlet radial position r to the core boundary R_o , where it is considered captured, and the right term over the entire length h , the following expression for the cyclone grade efficiency can be obtained:

$$\ln \left(\frac{R_o}{r} \right) = \frac{1}{2} \ln \left(\frac{1}{1-\eta} \right) = \left(\frac{\rho d \eta^2}{18\mu} \right) \left(\frac{\pi s^2}{R_o^2 h} \right) \left(\frac{Q_p^4}{Q^2 Q_s} \right) \left(\left\{ 1 + \frac{Q_s}{Q_p} \right\}^4 - 1 \right) \quad (14)$$

or

$$d\eta = \sqrt{\left(\frac{9\mu}{\rho} \right) \left(\frac{R_o^2 h}{\pi s^2} \right) \frac{Q^2}{1 + \frac{Q_s}{Q_p} - 1} \left(\frac{Q_s}{Q_p^4} \right) \left(\ln \left\{ \frac{1}{1-\eta} \right\} \right)} \quad (15)$$

TABLE 1. PREDICTED CYCLONE PERFORMANCE VS. CYCLONE SIZE

Cyclone	Primary flow Q_p (m ³ /s)	Secondary flow Q_s (m ³ /s)	Length h (cm)	Outside diam. OD (cm)	Core diam. R_o (cm)	d_o (μ)	d_{50} (μ)
#1	0.024	0.014	34	5.0	2.5	0.78	1.42
#2	0.183	0.113	42	16.2	8.1	1.0	1.81
#3	0.427	0.283	75	2.5	12.5	1.37	2.46

Gas viscosity—0.0002 poise.

Particle density—2.0 g/cm³.

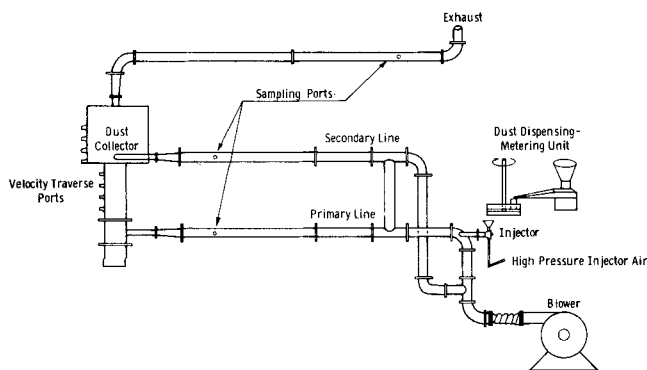


Fig. 2. Schematic of cyclone test apparatus.

This expression assumes a uniform distribution of particles over the entrance. Equations (11) and (15) can be used to predict the particle diameters for 50% (d_{50}) collection and zero collection (d_0) for comparison with published data. Table 1 has been prepared by using these equations for three commercially available rotary flow cyclones.

IMPLICATIONS

This simple model suggests a minimum particle size which can be collected in a rotary flow cyclone of about 1μ . The cut point varies with cyclone size but is around 1.9μ for the smallest (and most efficient) commercial unit. This contrasts sharply with the results of Klein (1963) but is consistent with the results of Dunson (1970) and Ogawa et al. (1972).

Klein (1973) claims rotary flow cyclone performance to be largely independent of gas temperature and unit size. Equations (11) and (15) suggest that performance is a function of gas viscosity, and, thus of gas temperature, with performance deteriorating as temperature increases. The equations also show that for a given gas/particle system the performance is dictated by a function with the form QS^2/R_0^2h . If the value of this group is maintained constant in cyclones of differing size, performance will be unaffected by the size change.

EXPERIMENTAL

Apparatus

A laboratory scale cyclone was purchased for experimental study. The cyclone body was 10 cm internal diam-

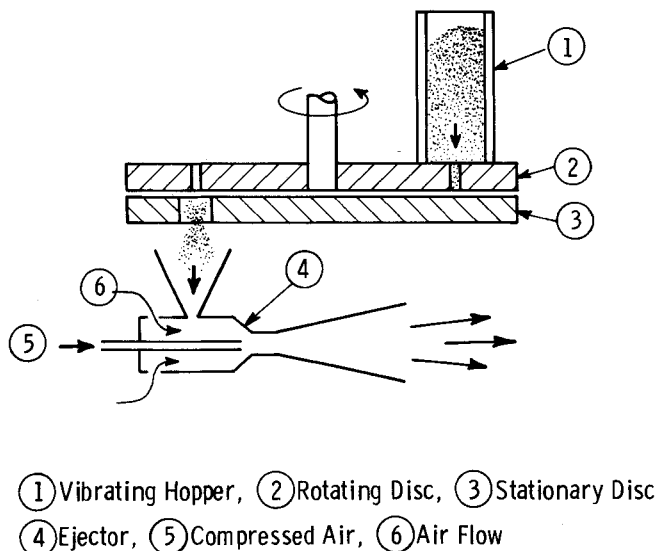


Fig. 3. Dust dispersion equipment.

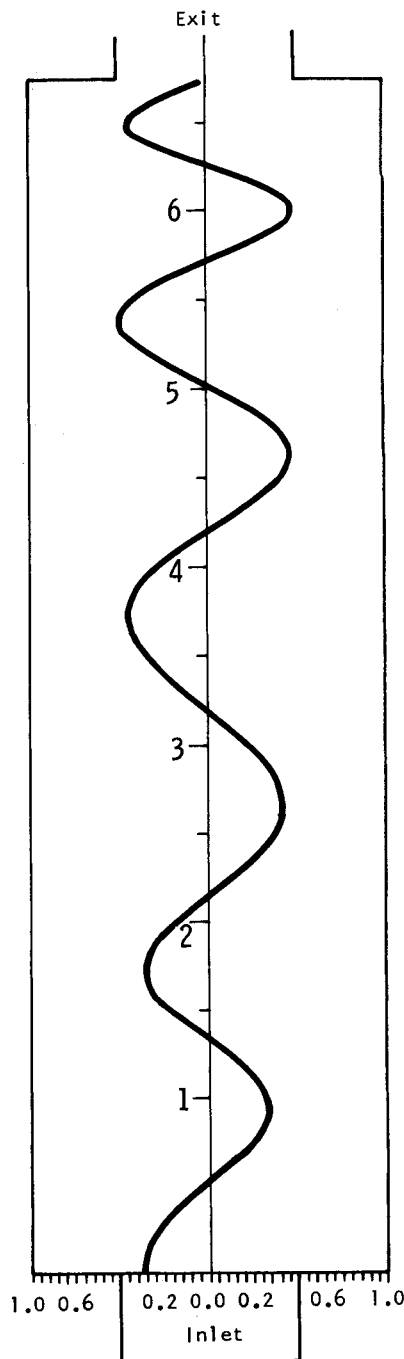


Fig. 4. A 10μ particle trajectory through the experimental cyclone under normal operating conditions.

eter, with a 5 cm diameter primary gas inlet and an inlet-to-outlet height of 34 cm. Secondary flow was directed by tangential nozzles as indicated in Figure 1. The design capacity of the unit was $0.024\text{ m}^3/\text{s}$ primary flow.

The test apparatus is shown in Figure 2. As indicated, the unit was fitted with a series of eight bosses along its length to allow pitot traverses to be made. Wedge probes were used for this purpose.

Provision of a controlled test dust dispersion proved difficult. The fine (-10μ) dust had a tendency to agglomerate, blocking vibratory feeders and dispersion equipment. These problems were overcome by using a modified Harvard dry dust disperser (Ciliberti and Lancaster, 1975). Dust was metered from a vibrating hopper into holes drilled in a rotating disk (Figure 3). Dust from the disk dropped into the suction tube of an ejector and was conveyed to the ejector chamber where a cross flow of air swept it into the high energy dispersion jet.

Dust loadings were determined by isokinetically sampling the streams and collecting the samples in thimble filters. Particle size distributions were measured by using cascade impactors.

TABLE 2. EXPERIMENTAL RESULTS

Test dust—10 μ limestone, 2 g/m³

Test gas—ambient air

Primary flow Q_p (m ³ /s)	Secondary flow Q_s (m ³ /s)	d_0 , μ	d_{50} , μ	Overall efficiency, %	Predicted efficiency, %
0.024 Dirty	0.014 Clean	2.3	2.5	60-65	81.4
0.024 Dirty	0.014 Dirty	2.3	2.8	61-66	
0.014 Dirty	0.024 Dirty	0.7	0.8	80-83	
0	0.024 Dirty	0.7	0.9	80-85	
0.014 Clean	0.024 Dirty	0.7	1.3	77-82	

Velocity Profile Measurements

Radial, axial, and tangential velocity profiles were determined in the experimental unit under various operating conditions. These measurements were used to calculate particle trajectories in the cyclone and to establish estimates of operating performance (Ciliberti and Lancaster, 1976). A typical calculated trajectory is shown in Figure 4. The data indicate that as the proportion of secondary flow is increased, the tangential velocity increases, which should improve unit performance. Increasing gas residence time by increasing the length of the cyclone body had the effect of broadening and lowering the axial velocity profile, causing relatively low tangential velocities in the region of the primary entrance. This also gave rise to flow instabilities. This mode of operation would be detrimental to collection efficiency.

EXPERIMENTS WITH TEST DUST

The dust collection was tested under five sets of operating conditions by using a -10 μ ground limestone test dust (Figure 5). The range of operating conditions and the test results are presented in Table 2.

The data indicate that when the cyclone is operated at its recommended flow rates, the performance is no better than that of a conventional cyclone of similar capacity (Jackson, 1963). However, by increasing the secondary gas flow rate, performance can be greatly improved. Performance was not substantially altered by use of a dirty secondary gas flow.

DISCUSSION

The simplified model for predicting cyclone performance is based on the assumption of a uniform flow of gas from the secondary flow region to the core of the cyclone. This assumption is supported both by our experimental observations of flow in a cyclone and those of Ogawa et al. (1972). The general nature of the equations suggests a steep grade efficiency curve, with a minimum collectable particle size. This corresponds well with our experimental observations and those of Dunson (1970) and Ogawa et al. (1972).

When the model was used to predict performance of actual cyclones, two assumptions were made. The inner core radius was assumed to be the same as that of the gas inlet, and the gas was assumed to make four revolutions in the core of the cyclone before reaching the exhaust. Experimental results show the core radius to be somewhat larger than that of the inlet over most of the cyclone length, while the number of revolutions in the core is four to five (for the small experimental cyclone considered). Consequently, the model gives an optimistic prediction of cyclone performance.

The use of experimental values for R_0 and S in Equations (11) and (15) produces estimated values for d_0 and d_{50} of 1.04 and 2.0 μ m, respectively. These may be compared with experimental values of 2.3 and 2.5 μ m (Figure 6).

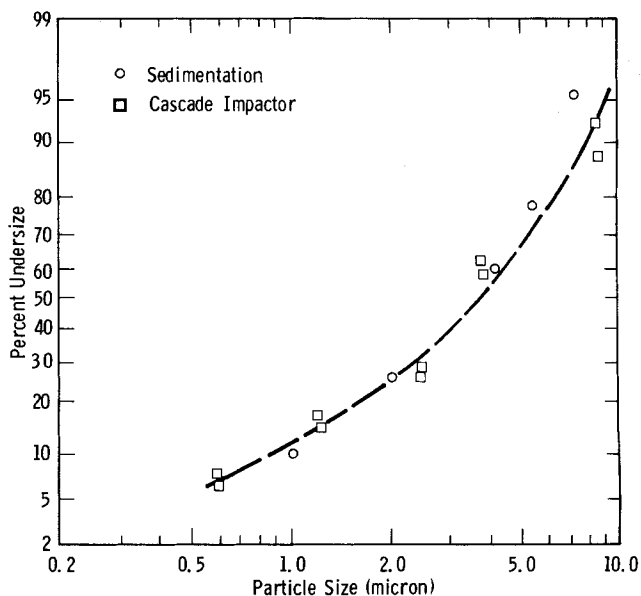
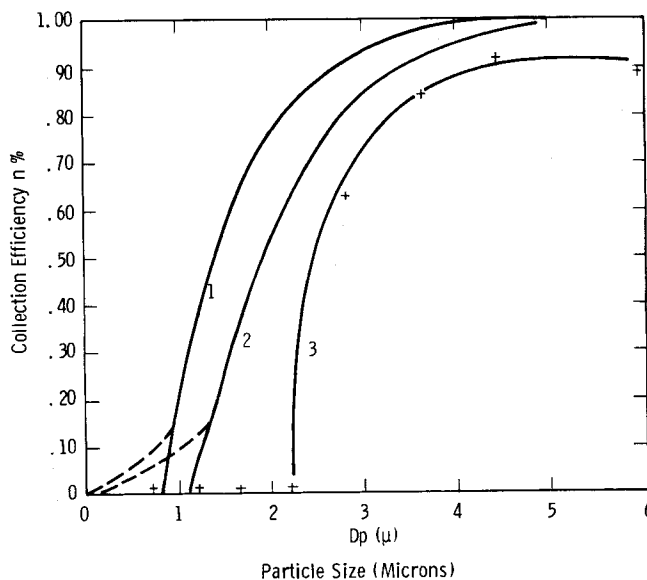


Fig. 5. Test dust size distribution.

Fig. 6. Experimental and predicted grade efficiency curves for rotary flow cyclone: 1. predicted by simple model, 2. predicted from model using experimental values of R_D & S , 3. experimental curve.

ACKNOWLEDGMENT

Financial support for this work was provided by the Energy Research and Development Agency under Contract E(49-L8)-1514.

NOTATION

d	= particle diameter
d_o	= minimum particle diameter collected
d_{50}	= diameter of particles collected with 50% efficiency
h	= length of cyclone body (inlet to outlet)
I	= moment of inertia
Q	= average gas flow rate in the core ($Q_p + Q_s/2$)
Q_p	= primary gas flow rate
Q_s	= secondary gas flow rate
Q_T	= total gas flow rate ($Q_s + Q_p$)
r	= radius
R_o	= radius of rotational flow core
s	= number of revolutions of gas flow in cyclone
t	= time
U_r	= particle radial velocity
V_t	= gas tangential velocity at R_o
V_z	= gas axial velocity
v_r	= gas radial velocity
v_t	= gas tangential velocity
Z	= axial distance from gas inlet

Greek Letters

η	= collection efficiency
μ	= gas viscosity
ρ	= particle density
ω	= gas angular velocity
ω_o	= gas angular velocity at inlet
θ	= angle

LITERATURE CITED

- Ciliberti, D. F., and B. W. Lancaster, "Modified 'Harvard' Dry Dust Dispenser," *Rev. Sci. Instr.*, **46**, 929 (1975).
- , "Fine Dust Collection in a Rotary Flow Cyclone," *Chem. Eng. Sci.* (1976).
- Dalla Valla, M. M., *United States Technical Conference on Air Pollution*, L. C. McCabe, ed., p. 341, McGraw-Hill, New York (1952).
- Dunson, J. B., "Dust Collector Performance Evaluation of Mid-get Impinger and Coulter Counter," Paper 5E, 63rd AIChE Annual Meeting, Chicago, Ill. (Nov., 1970).
- Friedlander, S. K., L. Silverman, P. Drinker, and M. W. First, *Handbook on Air Cleaning*, U.S.A.E.C. (AECD-3361; NYO-1572) (1952).
- Jackson, R., "The Performance of Cyclones," *B.C.U.R.A. Monthly Bulletin*, **27**, 413 (1963).
- Klein, Heinrich, "Entwicklung und Leistungsgrenzen des Drehstromungenstaubers," *Staub*, **23**, 501 (1963).
- , private communication, (Apr., 1973).
- Lucas, Robert L., in *Chemical Engineers' Handbook*, 5 ed., McGraw-Hill, New York (1973).
- Ogawa, A., K. Ikemori, M. Hirasawa, and K. Komuro, "On the Flow Pattern and the Cut Size of Particles in a Rotary Flow Dust Collector," *Japanese J. Powder Tech. Res.*, **9**, 371 (1972).
- Schmidt, Karl Ruldolph, "Physikalische Grundlagen Prinzip des Drehstromungenstaubers," *Staub*, **23**, 491 (1963).

Manuscript received September 3, 1975; revision received December 15 and accepted December 30, 1975.

ERRATA

P. S. Virk, "Drag Reduction Fundamentals," *AIChE J.*, **21**, 625 (1975).

Page	Col	Location	Should read:	Instead of:
626	2	line 1	4. Summary	SUMMARY
629	1	Fig. 2c caption	(5.5, 19)	(5.5, 10)
630	2	Fig. 5a legend	Whitsitt	Whittsitt
630	2	line 15	backbones	backbone
631	2	Sec. 1.1.6 line 7	40	38
		9	(triangles)	(hollow diamonds)
		10	30	300
		10	(hollow circles)	(triangles)
		11	110	100
631	2	Fig. 8 legend	Whitsitt	Whittsitt
633	1	Eqn. 12 RHS	\hat{B}	B
634	2	Sec. 2.1 line 5	originates	originotes
637	2	lines 15, 16, 17	.. example $v(Tw^*) = 100[\text{var}(Tw^*)]^{1/2}/Tw^*$, .. (same line, not broken up)	
637	2	line 22	$v(Tw^*)$	$\epsilon(Tw^*)$
		line 23	$v(\delta)$	$\epsilon(\delta)$
642		Table 4 title	MAXIMUM	MAXIM
647	2	Section 3.2 line 2	.. affected the affected by the ..
650	1	line -7	section	scetion
		line -3	(40)	(43)
652	2	line 2	seems	semes
652	2	Acknowledgements	index, H.	index. H.
653	2	Superscripts line 2	u_T and v	u_T and v
653	2	Other Symbols line 4	$v(\delta)$	$\epsilon(\delta)$

(Continued on page 414)